Crystal structure and vibrational spectra of hexagonal manganites YMnO$_3$ and LuMnO$_3$ under high pressure

View the article online for updates and enhancements.

IOP ebooks™

Bringing you innovative digital publishing with leading voices to create your essential collection of books in STEM research.

Start exploring the collection - download the first chapter of every title for free.

Materials Research Express

Crystal structure and vibrational spectra of hexagonal manganites YMnO$_3$ and LuMnO$_3$ under high pressure

S H Jabarov[1,2,3] , N T Dang[4], S E Kichanov[1], D P Kozlenko[1], L S Dubrovinsky[5], Je-Geun Park[6,7], Seongsu Lee[8], A I Mammadov[2], R Z Mehdiyeva[2], B N Savenko[1], N X Nghia[9], L H Khiem[9], N T T Lieu[10] and L T P Thao[11]

1   Frank Laboratory of Neutron Physics, Joint Institute for Nuclear Research, 141980 Dubna, Russia
2   Laboratory of Non-Standard Control and Diagnostics, Institute of Physics, ANAS, AZ-1143, Baku, Azerbaijan
3   Department of Physics and Technology, Azerbaijan State Pedagogical University, AZ-1000, Baku, Azerbaijan
4   Institute of Research and Development, Duy Tan University, 550000 Da Nang, Vietnam
5   Bayerisches Geoinstitut, University Bayreuth, D-95440 Bayreuth, Germany
6   Center for Correlated Electron Systems, Institute for Basic Science, 151-747 Seoul, Republic of Korea
7   Department of Physics and Astronomy, Seoul National University, 151-742 Seoul, Republic of Korea
8   Neutron Science Division HANARO, Korea Atomic Energy Research Institute, Daejeon 34057, Korea
9   Institute of Physics, Vietnam Academy of Science and Technology, Hanoi, Vietnam
10 Posts and Telecommunications Institute of Technology, Hanoi, Vietnam
11 University of Education, University of Da Nang, 550000 Da Nang, Vietnam

E-mail: sakin@jinr.ru and dangtoan2107@gmail.com

Keywords: crystal structure, high pressure, vibrational properties, multiferroics, perovskite

Abstract

The structural and vibrational properties of the multiferroics YMnO$_3$ and LuMnO$_3$ have been studied by means of the x-ray diffraction and Raman spectroscopy at high pressures up to 29.3 and 31.2 GPa, respectively. The initial hexagonal structure with space group $P6_3cm$ of both compounds remains unchanged in the entire pressure range. The anisotropic baric behaviors of lattice parameters and vibration modes of studied compounds were observed. The structural mechanisms of those phenomena are discussed.

1. Introduction

One of the topical problems of a current condensed matter physics is a study of the physical properties of novel multiferroic materials. The intrinsic property of such materials is a coupling between the magnetic and ferroelectric order parameters, resulting in the magnetoelectric effect and the possibility to control magnetic properties by an electric field and vice versa [1–3]. The multiferroic compounds have the application opportunities as the materials for microelectronics components, magnetic and electrical field sensors or data storage devices [4–6].

The manganites with general formula RMnO$_3$, where R is a rare-earth ion, crystallize in the orthorhombic structure with the *Pnma* space group, if the R element has a large ionic radius, like as La, Pr, Nd, Sm, Eu, Gd, and Tb [7]. In contrast, compounds with the smaller ionic radius of rare-earth elements (as Ho, Er, Tm, Yb, Lu, Y, Sc) have a hexagonal crystal structure with the polar $P6_3cm$ space group [8–10]. The particularly interesting feature of these compounds is a combination of multiferroic phenomena with the low dimensional magnetism of the geometrically frustrated triangular lattice, realized via giant magnetoelastic coupling [8, 9, 11]. The crystal structure of the hexagonal manganites consists of two-dimensional triangular lattices of Mn ions in *ab* planes, separated by noncoplanar layers of rare earth ions. The magnetic properties of the hexagonal systems demonstrate a strong dependence on the ionic radius r_R of the R element. Contrast to the absence of a long-range magnetic order in InMnO$_3$ with the largest value of r_R, YMnO$_3$ exhibits a long-range antiferromagnetic (AFM) order of Γ_1 or Γ_3 irreducible representation symmetry, whereas others with smaller r_R such as LuMnO$_3$ exhibit a different long-range AFM structure of Γ_2 or Γ_4 irreducible representation symmetry [8, 9, 12]. Interestingly, for both YMnO$_3$ and LuMnO$_3$ compounds around T_N it was observed sharp anomalies in dielectric constant and

loss tangent although the ferroelectric transition temperature of $T_C \approx 900$ K is much higher than T_N [13, 14]. Furthermore, the magnetic transition in both compounds $YMnO_3$ and $LuMnO_3$ is accompanied by an isostructural transition characterized by a contrast change of lattice parameters and an unusual large atomic displacement [11]. These arguments imply a strong coupling between electric, magnetic, and lattice degrees of freedom in the compounds.

An important insight into the relationship between the various competing factors and their particular role in formation of magnetoelectric properties of manganite compounds can be given by high pressure studies, exploring a response of physical properties on reduction of interatomic distances and corresponding valence angles. Moreover, it is expected that the magnetic frustration makes these hexagonal compounds very sensitive to small perturbations in parameters such as the magnetic field or pressure. It was found that the application of high pressure strongly suppresses the ordered Mn magnetic moments of $YMnO_3$ and $LuMnO_3$, implying enhanced spin fluctuations. Moreover, pressure-induced spin reorientation and a change in the symmetry of the AFM structure were observed in $YMnO_3$, while the AFM structure of $LuMnO_3$ remains unchanged under compression up to 6 GPa [8, 9, 12]. However, the structural and vibrational properties of $YMnO_3$ and $LuMnO_3$ at high pressure remain not well explored. A partial structural phase transition into the metastable orthorhombic phase in $YMnO_3$ at $P \sim 24$ GPa, and in $LuMnO_3$ at $P \sim 22$ GPa was recently reported [12, 15]. To clarify in more detail the high-pressure effects on the structural parameters and vibrational spectra of $YMnO_3$ and $LuMnO_3$, we have performed a study of both compounds by means of powder x-ray diffraction (XRD) and Raman spectroscopy methods in the extended pressure range up to ~30 GPa.

2. Experimental

The powder samples of $YMnO_3$ and $LuMnO_3$ were prepared by the typical solid phase reaction method as described in [8, 9, 12]. Oxides Y_2O_3 (Lu_2O_3) (99.999%) and Mn_2O_3 (99.999%) were thoroughly mixed. The obtained homogeneous mixture was heated up to 900 °C for 12 h, then it was successively annealed at temperatures of 1100 and 1200 °C for 24 h. After that, it was finally sintered at a temperature of 1350 °C for 24 h with intermediate grindings performed to prevent the formation of stable phases of minor impurities. An XRD analysis shows a pure hexagonal phase of $YMnO_3$ and $LuMnO_3$.

The XRD patterns were measured in the pressure range up to 25.7 GPa for $YMnO_3$, and up to 31.2 GPa for $LuMnO_3$, at room temperature using a specialized x-ray diffractometer. This diffractometer consists of an FRD high-flux x-ray emitter (Mo Kα radiation with wavelength $\lambda = 0.7115$ Å), a FluxMax focusing optical system, and the SMART APEX CCD detector [12]. For conversion of the 2D diffraction data to 1D patterns, we used the Fit2D program [16]. The diamond anvil cell of the design [17] was used. The diameter of the anvil culets was 300 μm. The sample was placed into a rhenium gasket with the hole diameter of 150 μm. As a pressure transmitting medium, we used a methanol-ethanol-water mixture with proportion of 15:3:1. The pressure in the cell was measured using the ruby luminescence with an accuracy of 0.05 GPa. For the additional pressure calibration, we placed a small piece of a gold wire inside the gasket. The XRD data were analyzed by the Rietveld method using the FullProf program [17].

Raman spectra at ambient temperature and pressures up to 30 GPa were collected using a LabRam spectrometer (NeHe excitation laser) with wavelength of 632.8 nm, 1800 grating, confocal hole of 1100 μm, and a 50× objective.

3. Results and discussion

3.1. X-ray diffraction

XRD patterns of $YMnO_3$ and $LuMnO_3$ measured at selected pressures and ambient temperature are shown in figure 1. At ambient and high pressures, they correspond to the hexagonal crystal structure with space group $P6_3cm$. The values of lattice parameters determined at ambient conditions are $a = 6.0616(5)$ Å, $c = 11.3939(7)$ Å for $LuMnO_3$ and $a = 6.1334(6)$ Å, $c = 11.3723(7)$ Å for $YMnO_3$, which are consistent with previous studies [8, 9, 12]. An absence of the extra peaks and qualitatively similar character of XRD data over whole studied pressure range imply structural stability of $YMnO_3$ and $LuMnO_3$. We assumed that, in whole pressure range in experiments, the hexagonal phase with space group $P6_3cm$ of both investigated compounds remains unchanged.

The pressure dependencies of lattice parameters of $YMnO_3$ and $LuMnO_3$ are shown in figures 2(a), (b). The lattice compression of both compounds is strongly anisotropic with the most compressible a and weakly compressible c lattice parameters. The relevant average compressibilities $k_i = -(1/a_{i0})(da_i/dP)_T$ are $k_a = 0.0015$, $k_c = 0.0007$ GPa^{-1} for $YMnO_3$ and $k_a = 0.0012$, $k_c = 0.0006$ GPa^{-1} for $LuMnO_3$, respectively.

The pressure dependent unit cell volumes of $YMnO_3$ and $LuMnO_3$ are shown in figures 2(c), (d). The volume compressibility data were fitted by the third-order Birch–Murnaghan equation of state [18]:
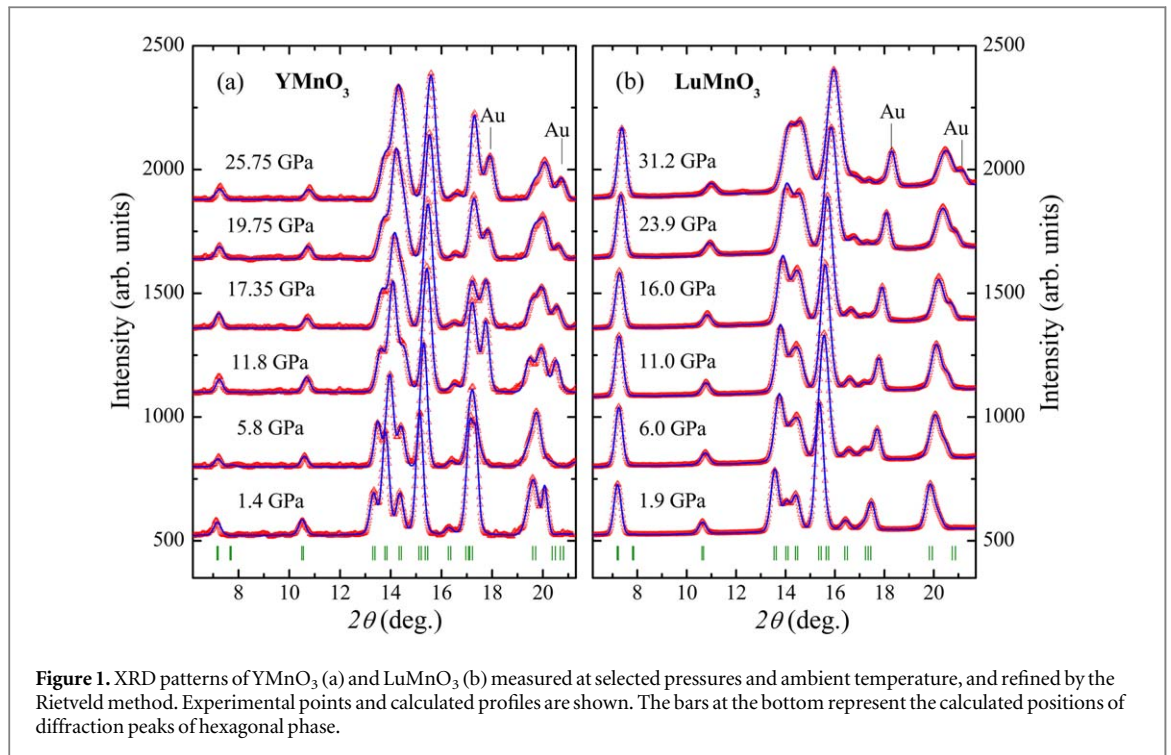
Figure 1. XRD patterns of YMnO$_3$ (a) and LuMnO$_3$ (b) measured at selected pressures and ambient temperature, and refined by the Rietveld method. Experimental points and calculated profiles are shown. The bars at the bottom represent the calculated positions of diffraction peaks of hexagonal phase.

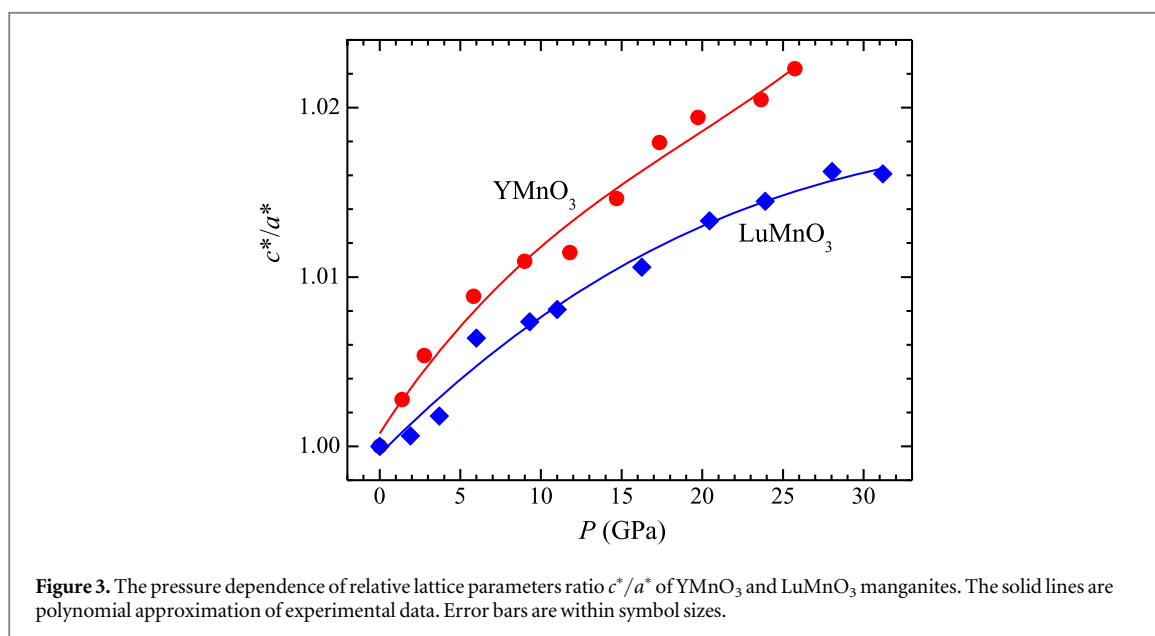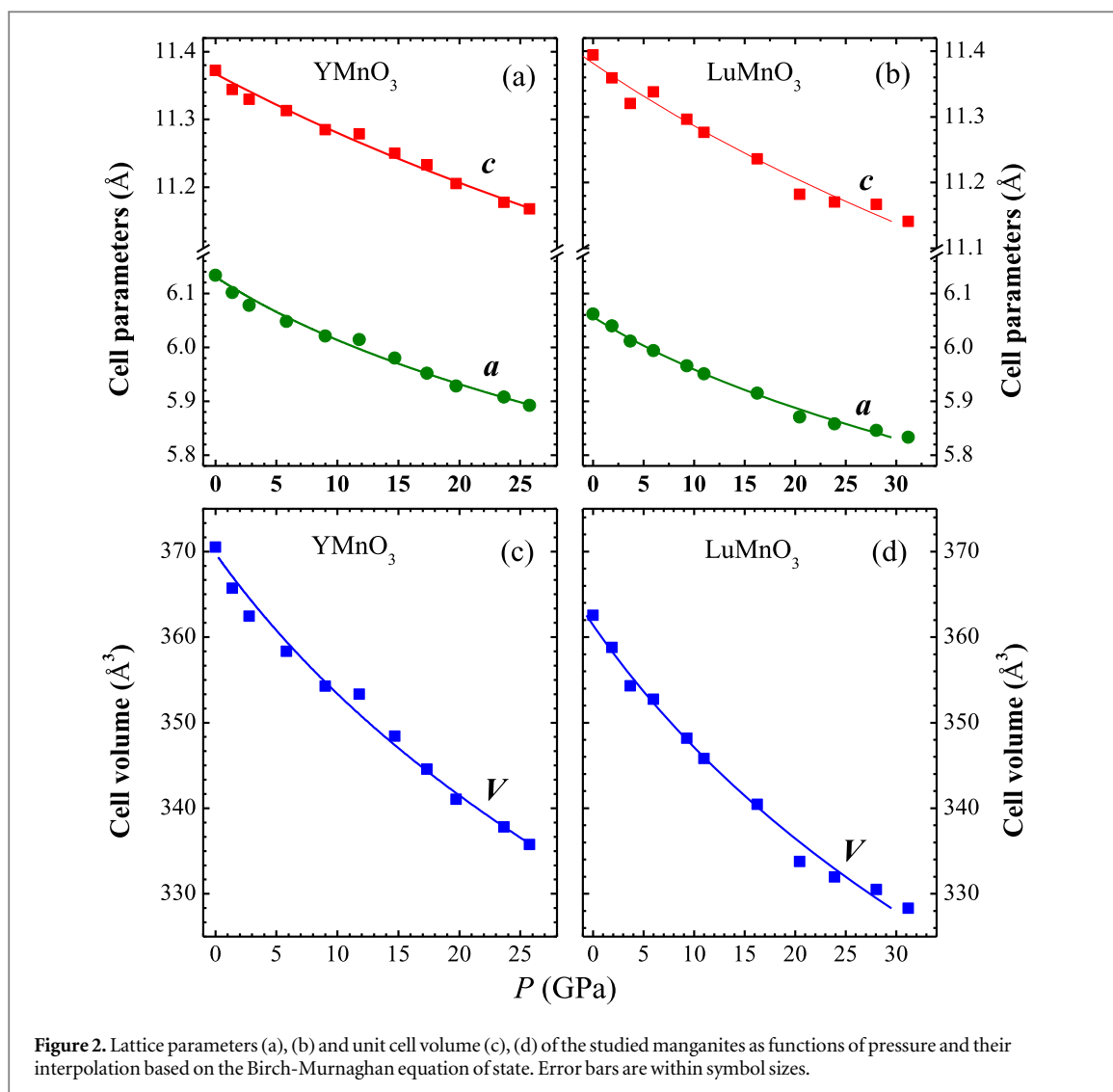$$P = \frac{3}{2} B_0 (x^{-7/3} - x^{-5/3}) \left[1 + \frac{3}{4} (B' - 4)(x^{-2/3} - 1) \right],$$

where $x = V/V_0$ is the relative volume change, V_0 is the unit cell volume at $P = 0$ GPa, B_0 and B' are the bulk modulus $B_0 = V(dP/dV)_T$ and its pressure derivative $B' = (dB_0/dP)_T$. The obtained values are $B_0 = 157(5)$ GPa and $B' = 12(2)$ for YMnO$_3$, and $B_0 = 180(6)$ GPa and $B' = 12(2)$ for LuMnO$_3$. For YMnO$_3$, the bulk modulus somewhat exceeds those of $B_0 = 112$ GPa, previously estimated for the more restricted pressure range up to about 17 GPa [15], while B' values are about the same. For LuMnO$_3$, in the study [15] unreasonably large value of $B' = 26$ was obtained, providing relatively small bulk modulus $B_0 = 109$ GPa. From our data, comparable values of $B' = 12$ are evaluated for both YMnO$_3$ and LuMnO$_3$.

The comparative presentation of the anisotropy in lattice compressibility of YMnO$_3$ and LuMnO$_3$ can be shown as pressure dependence of relative ratio of hexagonal axes: $a^* = a/a_0$ and $c^* = c/c_0$. The parameter c^*/a^* as a function of pressure demonstrates a faster growth for YMnO$_3$ in comparison with LuMnO$_3$ (figure 3). This fact can indicate more pronounced anisotropy of the lattice compression of YMnO$_3$, which can lead to drastic changes in the magnetic structure observed previously [8, 12].

3.2. Raman spectroscopy

The Raman spectra of YMnO$_3$ and LuMnO$_3$ measured at selected pressures and ambient temperature, are shown in figure 4. The group theoretical analysis for the phonon modes of studied hexagonal manganites gives 38 Raman-active modes at the Γ-point: $\Gamma_{Ram} = 9A_1 + 14E_1 + 15E_2$ [11]. In our Raman spectroscopy experiments, the five Raman lines are detected. The positions and tentative assignments of Raman lines are listed in table 1. The strong Raman line at ~692 cm^{-1} is assigned to apical oxygen stretching vibrations along the c axis of A_1 symmetry in Mn-O polyhedra. The neighboring weak line at ~644 cm^{-1}, observed in LuMnO$_3$ only, corresponds with (x, y) vibrations of in-plane oxygen atoms of E_2 symmetry. The mode at ~472 cm^{-1} can be assigned to (x, y) in-plane vibrations of the apical oxygen and Mn atoms of the A_1 symmetry [19, 20]. The presence of this A_1 mode, which is expected to be silent for the centrosymmetric $P6_3/mmc$ structure, implies that the crystal structure symmetry of YMnO$_3$ and LuMnO$_3$ remains polar in the studied pressure range. The vibration mode at ~310 cm^{-1} is associated to the relative displacements of the apical oxygen atoms along the c direction and the (x, y) displacements of one of the in-plane oxygen atoms of the E_2 symmetry [11, 20]. It reflects the Mn–O–O–Mn bond vibrations, which moderated the super-exchange Mn-Mn interaction between the adjacent Mn planes. The vibration mode A_1 at 264 cm^{-1} is associated to the displacements of Y/Lu and Mn atoms along the z axis [11, 19, 20].

One should note that in the metastable orthorhombic perovskite-like modification of YMnO$_3$, the Raman spectra exhibit strong Raman modes at 500 and 615 cm^{-1} [21], associated with the Jahn-Teller distortions of
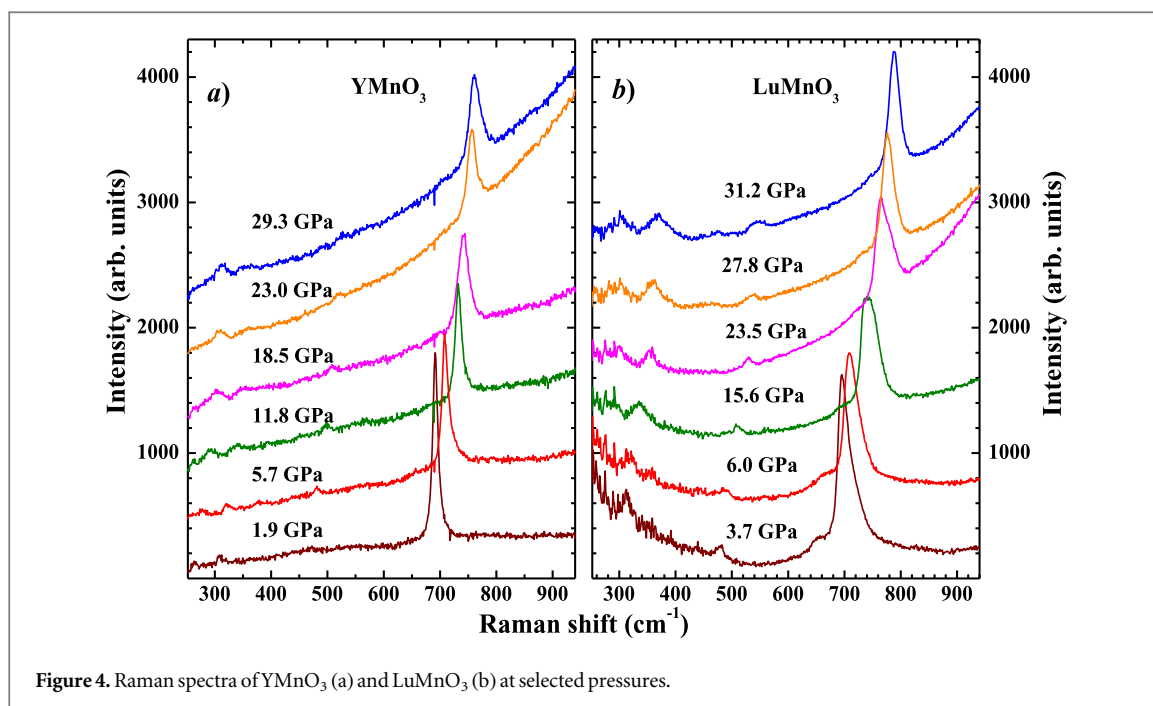
Figure 2. Lattice parameters (a), (b) and unit cell volume (c), (d) of the studied manganites as functions of pressure and their interpolation based on the Birch-Murnaghan equation of state. Error bars are within symbol sizes.

Figure 3. The pressure dependence of relative lattice parameters ratio c^*/a^* of YMnO$_3$ and LuMnO$_3$ manganites. The solid lines are polynomial approximation of experimental data. Error bars are within symbol sizes.

Figure 4. Raman spectra of $YMnO_3$ (a) and $LuMnO_3$ (b) at selected pressures.

Table 1. Raman frequencies of $YMnO_3$ and $LuMnO_3$ at 1.9 GPa. The pressure coefficients for the observed modes are also given.
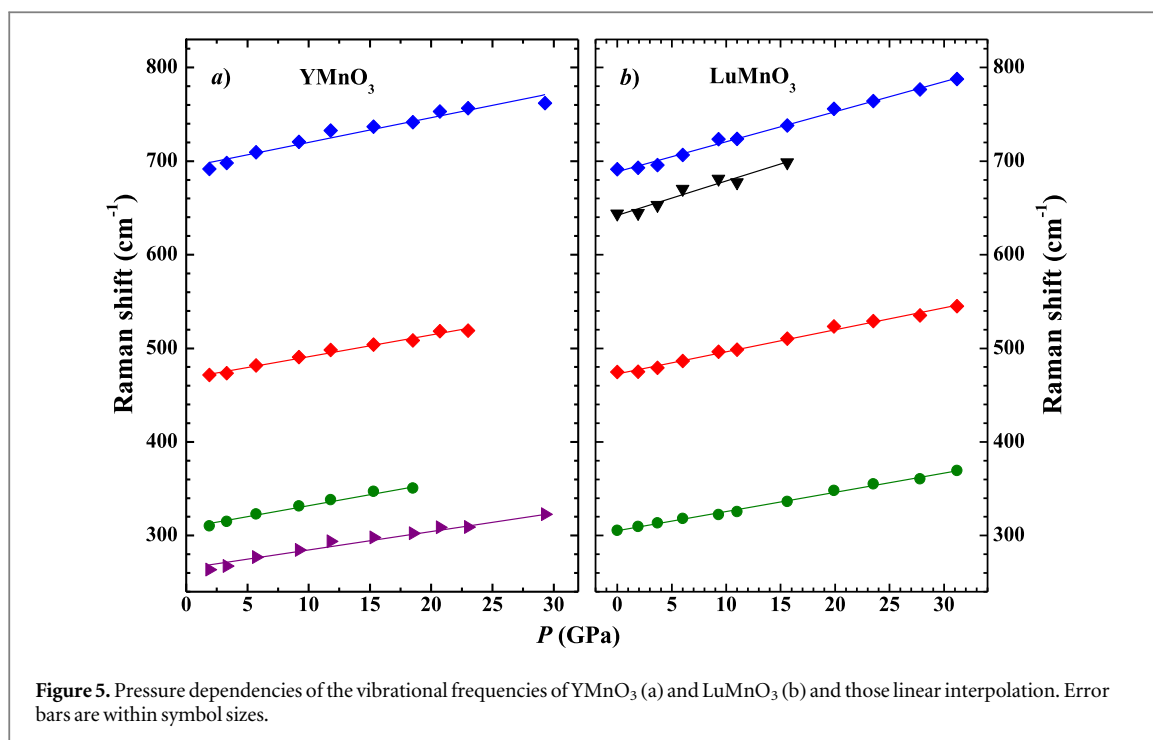
Assignment	YMnO₃ Mode (cm⁻¹)	YMnO₃ $k_{\nu i}$	LuMnO₃ Mode (cm⁻¹)	LuMnO₃ $k_{\nu i}$
A_1	263.6	0.0080	—	—
E_2	310.3	0.0081	309.5	0.0067
A_1	471.4	0.0050	474.9	0.0050
E_2	—	—	644.5	0.0057
A_1	691.6	0.0038	693.0	0.0047

MnO_6 octahedral units. The absence of the extra modes in the relevant frequency regions supports the stability of the hexagonal structural modifications of $YMnO_3$ and $LuMnO_3$ over the studied pressure range.

The pressure application results in an increase of all the vibrational frequencies as can be seen in figure 5. The pressure coefficients $k_{\nu i} = (1/\nu_{i0})d\nu_i/dP$ are the smallest for the A_1 apical oxygen stretching vibrations, being about 0.0038 and 0.0047 GPa^{-1} for $YMnO_3$ and $LuMnO_3$, respectively (table 1). This is consistent with the smallest compressibility of the *c*-axis, along which the apical Mn-O bonds are located. For the lower frequency A_1 and E_2 modes, the pressure coefficients increase up to 0.0080 GPa^{-1} (table 1), reflecting contribution from the more pronounced compressibility of the *a*-axis.

4. Conclusions

The XRD and Raman scattering analyses demonstrate a pronounced anisotropy of the lattice compression of the hexagonal manganites $YMnO_3$ and $LuMnO_3$, causing anisotropic response of the vibration modes involving atomic displacements either along the *c*-axis or in the (*ab*) plane. No signs of the structural phase transition to the orthorhombic modification were found. The presence of the A_1 vibrational modes associated with the displacements of Mn ions in the (*ab*) planes, which are Raman active for the polar $P6_3cm$ symmetry and expected to be silent for the non-polar $P6_3/mmc$ one, implies also that the crystal structure remains polar in the studied pressure range.

Figure 5. Pressure dependencies of the vibrational frequencies of YMnO$_3$ (a) and LuMnO$_3$ (b) and those linear interpolation. Error bars are within symbol sizes.

Acknowledgments

ORCID iDs

S H Jabarov ⓘ https://orcid.org/0000-0002-3153-5804

References

[1] Cheong S-W and Mostovoy M 2007 *Nat. Mater.* **6** 13
[2] Cohen R E 1992 *Nature* **358** 136
[3] Eerenstein W, Mathur N D and Scott J F 2006 *Nature* **442** 759
[4] Fiebig M 2005 *J. Phys. D: Appl. Phys.* **38** R123
[5] Kozlenko D P *et al* 2017 *J. Alloys Compd.* **695** 2539
[6] Kozlenko D P *et al* 2014 *J. Alloys Compd.* **585** 741
[7] Gilleo M A 1957 *Acta Crystallogr.* **10** 161
[8] Kozlenko D P, Kichanov S E, Lee S, Park J-G, Glazkov V P and Savenko B N 2005 *J. Exp. Theor. Phys. Lett.* **82** 193
[9] Kozlenko D P, Kichanov S E, Lee S, Park J-G, Glazkov V P and Savenko B N 2006 *J. Exp. Theor. Phys. Lett.* **83** 346
[10] Katsufuji T *et al* 2002 *Phys. Rev.* B **66** 134434
[11] Toulouse C *et al* 2014 *Phys. Rev.* B **89** 094415
[12] Kozlenko D P, Mirebeau I, Park J-G, Goncharenko I N, Lee S, Park J and Savenko B N 2008 *Phys. Rev.* B **78** 054401
[13] Huang Z J, Cao Y, Sun Y Y, Xue Y Y and Chu C W 1997 *Phys. Rev.* B **56** 2623
[14] Katsufuji T, Mori S, Masaki M, Moritomo Y, Yamamoto N and Takagi H 2001 *Phys. Rev.* B **64** 104419
[15] Gao P, Chen Z, Tyson T A, Wu T, Ahn K H, Liu Z, Tappero R, Kim S B and Cheong S W 2011 *Phys. Rev. B - Condens. Matter Mater. Phys.* **83** 1
[16] Hammersley A P, Svensson S O, Hanfland M, Fitch A N and Hausermann D 1996 *High Press. Res.* **14** 235
[17] Dubrovinskaia N and Dubrovinsky L 2003 *Rev. Sci. Instrum.* **74** 3433
[18] Birch F 1986 *J. Geophys. Res.* **91** 4949
[19] Iliev M N, Lee H-G, Popov V N, Abrashev M V, Hamed A, Meng R L and Chu C W 1997 *Phys. Rev.* B **56** 2488
[20] Vermette J, Jandl S, Mukhin A A, Ivanov V Y, Balbashov A, Gospodinov M M and Pinsard-Gaudart L 2010 *J. Phys. Condens. Matter* **22** 356002
[21] Iliev M N, Abrashev M V, Lee H-G, Popov V N, Sun Y Y, Thomsen C, Meng R L and Chu C W 1998 *Phys. Rev.* B **57** 2872